Chinese Journal of Chemical Engineering 81 (2025) 76–86

Contents lists available at ScienceDirect

Chinese Journal of Chemical Engineering

journal homepage: www.elsevier.com/locate/CJChE

Full Length Article

Acid-base regulation in duodenum by intestinal fluid secretion: A simulation study

Yulan Zhao [1,#], Yifan Qin [2,#], Xiao Dong Chen [1], Jie Xiao [1,*]

[1] School of Chemical and Environmental Engineering, College of Chemistry, Chemical Engineering and Materials Science, Soochow University, Suzhou 215123, China
[2] Department of Chemical Engineering and Biological Engineering, Monash University, Melbourne 3800, Australia

ARTICLE INFO

Article history:
Received 20 August 2024
Received in revised form
8 December 2024
Accepted 19 December 2024
Available online 7 March 2025

Keywords:
Mixing
Bioreactor
Computational fluid dynamics (CFD)
Acid-base environment
Intestinal physiology

ABSTRACT

Up to now, how the secretion modes of intestinal fluid (*i.e.,* pancreaticobiliary secretion and wall secretion) can regulate intestinal acid-base environment has not been fully understood. Understanding the regulation mechanism is not only of great significance for intestinal health but may also lead to optimized designs for bio-inspired soft elastic reactors (SERs). In this work, the mixing and reaction of acidic gastric juice and alkaline intestinal fluid in a 3D duodenum with moving walls were modelled. A unique feature of this model is the implementation of both pancreaticobiliary and wall secretion of intestinal fluid as boundary conditions. This model allowed us to quantitatively explore the influence of secretion modes on pH regulation. The results demonstrated that coexistence of both pancreaticobiliary and wall secretions is the key to maintain the average pH in the duodenum at about 7.4. Their coexistence synergistically promotes the mixing and reaction of acid-base digestion liquids and provides a suitable catalytic environment for lipase in the intestine.

1. Introduction

The acid-alkaline environment (pH) in the intestine should be properly regulated in order to maintain the health of the digestive tract. The pH level influences the digestion rate of food by controlling the activity of enzyme [1], and the dissolution behavior of drugs [2]. Inappropriate regulation may lead to various intestinal diseases, *e.g.,* intestinal motility disorders, duodenal ulcers and dyspepsia [3,4]. The pH level in the duodenum can be affected by multiple factors, *e.g.,* gastric emptying, intestinal movement and intestinal fluid secretion. Among them, the intestinal fluid secretion plays a dominant role [5]. There are two secretion modes, *i.e.,* pancreaticobiliary secretion and wall secretion. The former contains bile and pancreatic juice (pH 7.1 − 8.2) and is secreted from the opening at the confluence of the bile duct and pancreatic duct in the descending duodenum [4]. The alkaline intestinal fluid (pH 7.5 − 8) secreted by the wall is from the Brunner's gland and small intestinal gland. The Brunner's gland located in the submucosa primarily secretes alkaline mucus, which is composed of mucin, water and inorganic salts such as bicarbonate, sodium and potassium. Mucus is capable of lubricating and protecting the intestinal wall [6]. The small intestinal mucosa contains many deep crevices lined with glandular epithelium. Cells lining along the crevices form the intestinal glands, or crypts of Lieberkühn, and produce a large amount of water and electrolytes [7].

The impact of duodenal intestinal fluid secretion on the intestinal environment has been investigated in many experimental studies. The deacidification capabilities of different intestinal fluid secretions in pigs were compared by Glad *et al.* [8], where the pancreaticobiliary secretion was found to play a key role in neutralizing gastric acid in the duodenum. Similar evidence was observed by Dutta *et al.* [9,10]. In patients with pancreatic secretion disorders, the pH in the duodenal lumen is much lower than that in healthy people. However, with a different *in vivo* pH measurement method, the change in the intestinal pH environment caused by the impaired pancreatic secretion was found negligible [11]. Several studies focused on the effect of duodenal ulcer, which inhibited the secretion amount of digestive juice from the intestinal wall. It was found that the pH in the patients' intestine was lower, demonstrating the importance of wall secretion of intestinal fluid in the process of gastric acid neutralization [12–17]. However, a human

This article is part of a special issue entitled: IPIC3 published in Chinese Journal of Chemical Engineering.

* Corresponding author.
E-mail address: jie.xiao@suda.edu.cn (J. Xiao).

# These authors contributed equally to this work.

https://doi.org/10.1016/j.cjche.2024.12.014

experiment conducted by Bendtsen *et al.* [18] saw little difference between patients with duodenal ulcer and healthy people. Furthermore, a view proposed by Ainsworth *et al.* [19,20] stated that there was a compensatory relationship between pancreaticobiliary secretion and wall secretion. When wall secretion was inhibited by hormones, the concentration of secretin in human serum increased, stimulating the secretion of bile and pancreatic juice. Although reported efforts improved our understanding of the acid-base regulation in the intestine, there are many questions remain unanswered. Are pancreaticobiliary secretion and wall secretion equally important? If yes, how do they synergistically regulate pH in the intestine? Why did some existing experimental studies report contradictory results? *In vivo* experiments were not capable of measuring the real-time evolution of pH distribution in the entire duodenum due to the operational complexity and ethical issues. Did the difference in measurement locations in different studies lead to contradictory conclusions?

In-vitro biomimetic models offer an effective way to explore the human digestive tract. The function of pancreaticobiliary secretion has been simulated in several *in-vitro* intestinal models, *e.g.,* TinyTIM [21], dDuo [22], and a bio-inspired soft elastic reactor [23]. An *in-vitro* semi-biomimetic intestinal model with pancreaticobiliary secretion was designed by resorting to the pancreatic lobular tube tissue of guinea pigs [24]. However, the secretion function on the intestinal wall is hard to be reproduced *in vitro*. The biomimetic models have been mainly used for drug solubility test and food digestion experiment. Buffer systems such as phosphate and acetate were often designed to keep intestinal environment pH at a fixed value [2]. Under physiological conditions, the neutralization capacity comes from the bicarbonate in the intestinal fluid. The pH is dynamically changed under the influence of factors such as intestinal motility, intestinal fluid secretion rate and secretion mode [25–27]. Therefore, the influences of the two intestinal secretion modes on the intestinal environment cannot be explored with the existing *in-vitro* biomimetic systems.

In-silico experiments are promising in addressing the limitations of *in-vivo and in-vitro* experimental studies listed above. Compared with *in-vivo* experiments, computer simulations can offer dynamic tracking of the process, which can capture the spatially and temporally distributed information on fluid flow and mass concentration. Compared with *in-vitro* digestive models, simulation models can implement certain complex structures and functions, such as various secretion modes and versatile motilities of the wall. For instance, by establishing a 2D duodenum model, the process of secreting digestive enzymes by the intestinal wall was simulated. The results verified that the wall secretion could promote the mixing of digestive enzymes and intestinal fluid [28]. By establishing a 3D gastrointestinal model, the reaction between digestive juices were simulated. Also, the impact of digestive juice secretion dysfunction on the intestinal pH was investigated [29,30]. The pore structure of the pancreaticobiliary opening was considered in this model. The major duodenal papilla, *i.e.,* the pancreaticobiliary port, is a small hole with a diameter of about 2 − 5 mm [31]. Intestinal fluid flows into the intestinal cavity through this hole, which influences the mass transfer, mixing and reaction of fluids in the intestine. Previous studies focused on either pancreaticobiliary secretion or wall secretion. The significance of coexistence of two secretion modes and their respective contributions to neutralizing gastric acid remain unknown. Also, the mechanism of acid-base regulation through intestinal fluid secretion in the duodenum has not been explored.

This work aims at quantitatively assessing the respective contribution of each secretion mode to the intestinal digestive environment. A 3D duodenum model that features both pancreaticobiliary secretion and wall secretion was developed. The gastric emptying of acidic solution and the periodic segmentation movement of the intestinal wall were taken into account. By tracking distributions of pH and enzyme activity in the intestine, the impact of intestinal fluid secretion mode on the intestinal environment was quantitatively analyzed to deepen our understanding of intestinal pH regulation, which is critical for the intestinal health.

2. Modeling and Simulation Methods

2.1. Geometry construction

The duodenum is modelled as a 3D rocket-shaped tube with a prespecified length L (m), as illustrated in Fig. 1(a). The geometry of the real duodenum in the human body is curved, often in the shape of a “C" or “L" [5]. As a first approximation, it is simplified as a straight tube, which is an assumption commonly adopted by previous computational fluid dynamics (CFD) models, as stated in the review article by Palmada *et al.* [32]. We improved the conventional straight tube geometry by implementing an axial-location-dependent tube radius. In this way, the realistic small opening of pylorus can be captured. The new geometry can offer a smooth transition from this small opening to the bulk lumen of the duodenum. While the current geometry does not fully capture the anatomical complexity of the duodenum, it remains representative and capable of reproducing the key physiological phenomena under investigation.

In consideration of the gap between the pylorus radius r_1 (m) and the duodenum radius R_0 (m), a transition segment of length l_1 (m) is constructed in the front end of the model. A circular hole for the injection of bile and pancreatic juice is located on the wall of the duodenum. According to the anatomy data, the axial distance from the pylorus to the hole is l (m), and the radius of the hole is r_2 (m). The geometric parameters are listed in Table 1.

2.2. Governing equations

The digestive phenomenon in the duodenum is extremely complex. It is very difficult to model the mass transfer and reactions of all components involved *in vivo*. As a first step towards a comprehensive understanding of digestive environment, this simulation mainly focuses on the transport and reaction of the secreted electrolytes in the water.

2.2.1. Momentum transfer

The flow in the duodenum is a laminar flow of an incompressible fluid [41], which can be described by the continuity equation and the Navier-Stokes equation:

$$\frac{\partial \rho}{\partial t} + \nabla \cdot (\rho \boldsymbol{u}) = 0 \tag{1}$$

$$\frac{\partial}{\partial t}(\rho \boldsymbol{u}) + \nabla \cdot (\rho \boldsymbol{u}\boldsymbol{u}) = -\nabla p + \nabla \cdot \left[\mu \left(\nabla \boldsymbol{u} + (\nabla \boldsymbol{u})^{\mathrm{T}} \right) - \frac{2}{3}\mu (\nabla \cdot \boldsymbol{u}) \boldsymbol{I} \right] \tag{2}$$

where ρ is the fluid density ($\mathrm{kg \cdot m^{-3}}$), $\boldsymbol{u}$ is the velocity vector of fluid ($\mathrm{m \cdot s^{-1}}$), p is the fluid pressure (Pa), μ is the fluid viscosity (Pa·s), $\boldsymbol{I}$ is the unit tensor, and t is the time (s).

2.2.2. Mass transfer

The species in the fluid involves hydrochloric acid, sodium bicarbonate, sodium chloride, carbon dioxide. The mass fraction of each component follows the transport equation below:

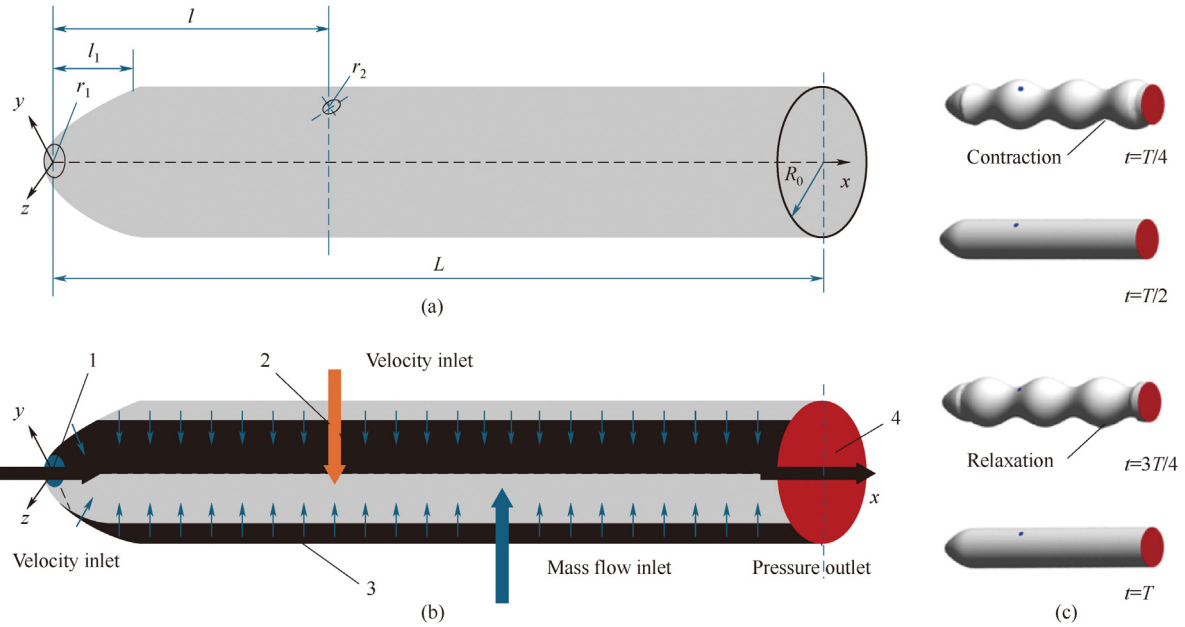

Fig. 1. 3D duodenum model with (a) its geometry and (b) boundary conditions and (c) its shape change in one cycle of segmentation movement. In subplot (b), 1 and 4 are the duodenal inlet and outlet, respectively. 2 refers to the pancreaticobiliary port. 3 refers to the intestinal wall that secrets intestinal fluid.

Table 1
Parameter values used in the 3D duodenum model.

Parameters		Notation	Values	References
Geometry	Pylorus radius	r_1	4.63×10^{-3} m	[33]
	Pancreaticobiliary port radius	r_2	2.5×10^{-3} m	[31]
	Duodenum radius	R_0	0.02 m	[34]
	Duodenal length	L	0.25 m	[34]
	Transition segment length	l_1	3×10^{-4} m	[33]
	Axis distance from pancreaticobiliary port and the pylorus	l	0.1 m	[33]
Segmentation motility	Amplitude	ε	25%	[35]
	Frequency	f	0.1667 s^{-1}	[34]
	Wavelength	λ	7×10^{-2} m	[36]
Secretion at the duodenal inlet	Initial concentration	$c_{1,H}$	10 $mol \cdot m^{-3}$	[2]
	Volumetric flow rate	F_g	1.667×10^{-7} $m^3 \cdot s^{-1}$	[33]
Wall secretion	Initial concentration	$c_{w,N}$	10 $mol \cdot m^{-3}$	[15]
	Rate of produced bicarbonate	Q_w	8.333×10^{-7} $mol \cdot s^{-1}$	[15]
Pancreaticobiliary secretion	Initial concentration	$c_{p,N}$	40 $mol \cdot m^{-3}$	[37]
	Sodium bicarbonate output	Q_p	2.778×10^{-6} $mol \cdot s^{-1}$	[15]
Diffusion coefficients	Hydrochloric acid	D_{HCl}	7×10^{-9} $m^2 \cdot s^{-1}$	[38]
	Sodium bicarbonate	D_{NaHCO_3}	1.75×10^{-9} $m^2 \cdot s^{-1}$	[38]
	Sodium chloride	D_{NaCl}	2.5×10^{-9} $m^2 \cdot s^{-1}$	[38]
	Carbon dioxide	D_{CO_2}	2.47×10^{-9} $m^2 \cdot s^{-1}$	[38]
Reaction rate constant		k	1×10^4 $m^3\ mol^{-1} \cdot s^{-1}$	[39]
Dissociation constant of carbonic acid		K_1	4.9×10^{-4} $mol \cdot m^{-3}$	[30]
		K_2	5.62×10^{-7} $mol \cdot m^{-3}$	[30]
The ionic product constant of water		K_w	1×10^{-8} $mol^2 \cdot m^{-6}$	[30]
First and second lipase dissociation constants (equal to $-\lg(K_{a1})$ and $-\lg(K_{a2})$)		pK_{a1}	5.8	[40]
		pK_{a2}	10.1	[40]

$$\rho \frac{\partial Y_i}{\partial t} + \nabla \cdot (\rho \boldsymbol{u} Y_i) = -\nabla \cdot J_i + S_i \tag{3}$$

where Y_i is the mass fraction of component i in a multi-component mixture. J_i represents the diffusion flux of component i. In a thermostatic digestive system, the diffusion rate is only dependent on the concentration gradient. The intensity vector due to molecular diffusion process can be expressed by Eq. (4):

$$J_i = -\rho D_{i,m} \nabla Y_i \tag{4}$$

where $D_{i,m}$ is the diffusion coefficient of component i, $m^2 \cdot s^{-1}$. Their values are given in Table 1.

S_i in Eq. (3) represents the generation or consumption rate of each component. The reaction of sodium bicarbonate and hydrochloric acid in the duodenum is irreversible [39,42]. The chemical equation is:

$$HCl + NaHCO_3 \xrightarrow{k} CO_2 + NaCl + H_2O$$

In a thermostatic system, the rate of the neutralization reaction is proportional to the product of hydrochloric acid and sodium hydrogen carbonate concentrations:

$$S_i = M_i k c_{HCl} c_{NaHCO_3} \tag{5}$$

$$c_i = \frac{\rho Y_i}{M_i} \tag{6}$$

where k is the reaction rate constant ($m^3 \cdot mol^{-1} \cdot s^{-1}$). c_i is the concentration of component i ($mol \cdot m^{-3}$). which can be calculated by Equation (6). M_i is the molecular weight of component i ($g \cdot mol^{-1}$). The saturated solubility of carbon dioxide under physiological conditions is 25 $mol \cdot m^{-3}$ [27]. The maximum concentration of carbon dioxide in this work is 6 $mol \cdot m^{-3}$, which indicates that carbon dioxide dissolves completely in the intestinal fluid.

2.3. Initial and boundary conditions

The initial and boundary conditions for the duodenum model are shown in Fig. 1(a) and (b). The initiation of the simulation is a tube filled with water only. The duodenum is a multi-opening lumen. To simulate the emptying of gastric acid, the fluid containing hydrochloric acid is injected from the inlet 1, *i.e.*, the pylorus. In most cases, the rate of gastric emptying evolves with time [43]. In this simulation, the research emphasis is the secretion mode of intestinal fluid, so the injection rate of gastric content is controlled to be a constant. The flow velocity of the acidic fluid at inlet 1 (v_1) can be computed by:

$$v_1 = \frac{F_g}{\pi {r_1}^2} \tag{7}$$

where F_g is the volumetric flow rate of gastric juice at the duodenal inlet ($m^3 \cdot s^{-1}$). Wall contraction of stomach results in the volumetric flow rate, about 8–10 $ml \cdot min^{-1}$ [33]. $c_{1,H}$ is the initial concentration of hydrochloric acid in gastric juice secretion ($mol \cdot m^{-3}$). And the concentration of hydrochloric acid at the pylorus is set to 10 $mol \cdot m^{-3}$, corresponding to a pH value of 3 [2].

The pancreaticobiliary port (*i.e.*, inlet 2) secretes pancreatic juice and bile, which contains diverse enzymes and electrolytes in reality. As the aim of this study is to investigate the *in-vivo* acid-base environment, enzymes are not taken into account herein. Furthermore, only sodium bicarbonate is simulated herein, which is the major alkaline electrolyte in the pancreaticobiliary secretion [15]. The velocity v_p of intestinal fluid secreted at the pancreaticobiliary port is defined ($m \cdot s^{-1}$). It can be calculated based on the bicarbonate secretion rate Q_p ($mol \cdot s^{-1}$), bicarbonate concentration $c_{p,N}$ ($mol \cdot m^{-3}$) and the area of the secretion port.

$$v_p = \frac{Q_p}{\pi {r_2}^2 c_{p,N}} \tag{8}$$

Similarly, the intestinal wall is assumed to secrete bicarbonate aqueous solution only. The flux of bicarbonate secretion from the wall F_w ($mol \cdot m^{-2} \cdot s^{-1}$) can be defined by the formula below:

$$F_w = \frac{Q_w M_{NaHCO_3}}{Y_{w,N} A_w} \tag{9}$$

where Q_w is the rate of bicarbonate produced from the intestinal wall ($mol \cdot s^{-1}$). A_w is the effective area of wall secretion region (m^2). It is equivalent to the inner surface area of the cylinder excluding the area of pancreaticobiliary port, as shown in Fig. 1(a). M_{NaHCO_3} is the molecular mass of sodium bicarbonate ($kg \cdot mol^{-1}$). $Y_{w,N}$ is the mass fraction of sodium bicarbonate in the wall secretion, which can be calculated by $c_{w,N}$ according to Eq. (6). The parameter values for each boundary condition are illustrated in Table 1. Absorption of water and electrolytes through the intestinal wall is not considered.

In this study, two extreme cases were also designed: pancreaticobiliary secretion only (see Fig. 2(b)) and wall secretion only (see Fig. 2(c)). As shown in Table 2, the total sodium bicarbonate secretion rate for each case is controlled to be identical so as to evaluate the impact of different secreation scenarios. This assumption is reasonable given the compensatory mechanism between duodenal wall secretion and pancreaticobiliary secretion, which is regulated neurally [4,5]. This mechanism ensures adequate alkalinity to neutralize acidic components entering the duodenum, even if one mode of secretion is impaired. Ainsworth *et al.* [20] demonstrated this mechanism by using indomethacin to inhibit bicarbonate secretion from the duodenal wall. While the compensatory effect may not completely maintain a constant total secretion, our model's assumption serves as a reasonable approximation. Also in this simulation, the bicarbonate secretion rates (Q_p and Q_w) are assumed to remain constant over time. A study by You *et al.* [44] demonstrated that, in normal subjects, the bicarbonate secretion rate shows a slight increase over an extended period (*e.g.*, 240 min). However, given the relatively short simulation time (20 min) in this work, this variation is considered negligible. One should note that in reality, bicarbonate secretion rates are regulated by various mechanisms, including oral stimulation, gastric emptying, and intestinal physiology [6]. Consequently, the outcomes of a short-term simulation using a steady secretion rate may not accurately represent the mixing behavior throughout the entire digestion process. Additionally, the inflow rate of gastric juice should be dynamically adjusted based on the pressure difference between the stomach and the duodenum. Without a stomach

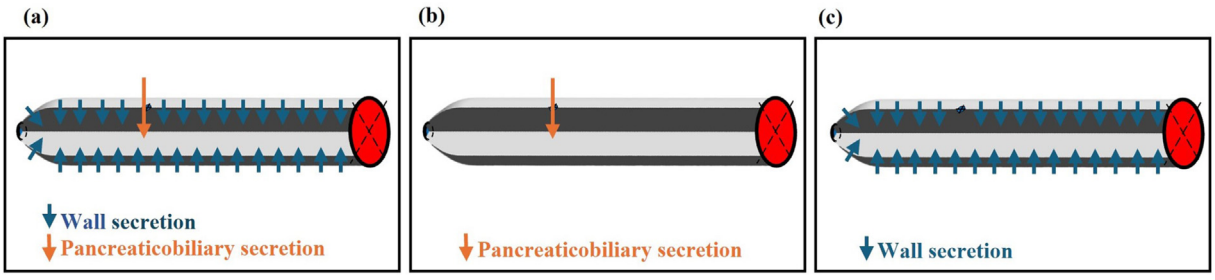

Fig. 2. Boundary conditions for different cases: (a) base case, (b) pancreaticobiliary secretion only, (c) wall secretion only.

Table 2
Model Settings for different cases.

Number	Case	Q_p/mol·s^{-1}	Q_w/mol·s^{-1}
1	Base case	8.333×10^{-7}	2.778×10^{-7}
2	Pancreaticobiliary secretion only	3.611×10^{-6}	–
3	Wall secretion only	–	3.611×10^{-6}

model, it is impossible to account for reflux phenomena in certain cases. It is important to note that Base case is set based on human physiological data, from the results of some clinical trials by Wolosin *et al.* [15].

As mentioned above, there may be a synergistic effect from both pancreaticobiliary and wall secretions. It is important to identify the appropriate range of secretion rate ratio from two secretion locations. This information can be used to tell the possibility of certain gastrointestinal diseases, since if the optimal range of secretion rate ratio is not achieved, the acid-base environment in the lumen will become unacceptable, leading to the risk of gastrointestinal diseases. This may help clinical management of gastrointestinal disorders. In addition to the two extreme cases, Case 1, Case 2, Case 4, Case 5, Case 6, Case 7, and Case 8 are also set, with their Q_p/Q_w values being 12.5/0.5, 12/1, 8/5, 6.5/6.5, 5/8, 3/10, and 1/12, respectively. On the basis of the data of Base case (Q_p/Q_w is 3/10) [15], one can change the ratio of secretion rates from two secretion locations, while keeping the total secretion rate of sodium bicarbonate unchanged, based on the compensation mechanism between the duodenal wall secretion and pancreaticobiliary secretion mentioned above.

Segmentation is the main form of intestinal motility that promotes the mixing in the duodenum. As shown in Fig. 1(c), this movement leads to ring-shaped contractions at fairly regular intervals along the gut, which are gradually replaced by another set of contractions in the previous relaxing sections. Contraction and relaxation occur sequentially at the same location, moving chyme forward and backward cyclically [45]. The wall displacement at any given time is described by a sinusoidal wave, effectively simulating the contraction and relaxation cycles.

$$P(x) = -\varepsilon R_0 \sin\left(\frac{2\pi}{\lambda}x\right), x \in [X_{\min}, X_{\max}] \tag{10}$$

where ε is the percentage of amplitude; R_0 represents the radius of duodenum outlet at rest (m); λ is the wavelength (m). $X_{\min}$ and $X_{\max}$ indicate the start and end positions of the contraction wave of segmentation movement, respectively (m). The segmentation movement of the intestinal wall is periodic with a certain frequency (Eq. (11)):

$$P(x,t) = -\varepsilon R_0 \sin\left(\frac{2\pi}{\lambda}x\right)\sin(2\pi f t), x \in [X_{\min}, X_{\max}] \tag{11}$$

where f is the frequency of segmentation movement (s^{-1}). The shortest distance from any point of the intestinal wall to the duodenal central axis can be obtained. That is, the radius after wall contraction is represented by Eq. (12):

$$R = R_0 - \varepsilon R_0 \sin\left(\frac{2\pi}{\lambda}x\right)\sin(2\pi f t), x \in [X_{\min}, X_{\max}] \tag{12}$$

2.4. Quantification of digestive environment

The digestion rate of starch in the duodenum depends heavily on the pH level. The activity of amylase is greatly affected by the acidity and alkalinity of the intestinal lumen environment [46]. According to the formulas derived by Kamaltdinov *et al.* [30], pH value can be expressed by a piecewise function depending on a concentration value of the substrate which is in excess.

$$\mathrm{pH} = \begin{cases} -\lg(c_{\mathrm{HCl}}) & \text{if } c_{\mathrm{HCl}} \geq c_{\mathrm{NaHCO_3}} \\ -\lg\left(\sqrt{\dfrac{K_1 \times (K_2 \times c_{\mathrm{NaHCO_3}} + K_w)}{K_1 + c_{\mathrm{NaHCO_3}}}}\right) & \text{if } c_{\mathrm{HCl}} < c_{\mathrm{NaHCO_3}} \end{cases} \tag{13}$$

where K_1 and K_2 are the dissociation constants of the carbonic acid (mol·m^{-3}). K_w is the ionic product constant of water (mol^2·m^{-6}).

The volume-averaged pH in the duodenal lumen is:

$$\overline{\mathrm{pH}} = \frac{\int (\mathrm{pH})\mathrm{d}V}{\int \mathrm{d}V} = \frac{\sum_{j=1}^{N}\left((\mathrm{pH})_j \times V_j\right)}{\sum_{j=1}^{N}(V_j)} \tag{14}$$

The pH-dependent activity of the enzyme corresponds to the ratio of the equivalent enzyme concentration for a specific pH level to the total enzyme concentration. The variation in the activity can be linked by the linearized form of the Michaelis function [40]:

$$\sigma = \frac{E^{\mathrm{pH}}}{E} = \frac{1}{1 + 10^{-\mathrm{pH}}/K_{a1} + K_{a2}/10^{-\mathrm{pH}}} \tag{15}$$

where σ is pH-dependent enzyme activity. K_{a1} and K_{a2} are the first and second dissociation constants of the enzyme respectively.

Similarly, the volume-averaged activity ($\overline{\sigma}$) of the enzyme is obtained:

$$\overline{\sigma} = \frac{\int \sigma \mathrm{d}V}{\int \mathrm{d}V} = \frac{\sum_{j=1}^{N}(\sigma_j V_j)}{\sum_{j=1}^{N}(V_j)} \tag{16}$$

The amount of sodium bicarbonate at the time of t can be obtained as well. The sodium bicarbonate in the simulation consists of three portions: the amount consumed by the neutralization reaction (n_α), escaped from the duodenal outlet (n_τ) and remained in the intestinal lumen (n_β):

$$n_\alpha = n_t - n_\tau - n_\beta \tag{17}$$

$$n_\tau = \int_0^t (F_\tau \overline{c}_\tau)\mathrm{d}t \tag{18}$$

$$n_\beta = \overline{c}_\beta \int \mathrm{d}V = \overline{c}_\beta \sum_{j=1}^{N}(V_j) \tag{19}$$

where F_τ (m^3·s^{-1}) and $\overline{c}_\tau$ (mol·m^{-3}) are the volumetric flow rate of intestinal fluid and the average concentration of sodium bicarbonate at the duodenal outlet, respectively. $\overline{c}_\beta$ (mol·m^{-3}) is the average concentration of sodium bicarbonate in the lumen.

2.5. Computational settings

The meshing and simulation were conducted using ANSYS Fluent. SIMPLE is used in the pressure velocity coupling algorithm for the transient flow problem. A user defined function (UDF) was

compiled to implement the wall motion based on Eq. (12). The adjustment of grid cells was conducted using dynamic mesh method specifying diffusion smoothing and automatic remeshing. The residuals of all equations were set to 0.0001. The time step for each system was 0.05 s. Under these configurations, the convergence requirement could be met in each time step. Simulation results were processed by ANSYS CFD-post and MATLAB.

3. Results and Discussion

3.1. Mesh independence analysis

Mesh independence studies were carried out by testing five different grid schemes. The number of cells were 40326, 61165, 86347, 132511 and 150562, respectively. Unstructured triangular mesh was employed. The average velocity, concentration of sodium bicarbonate and pH value were selected for mesh comparison. Though the digestion in the intestinal cavity is a long process, usually lasting several hours, this study simulates only the initial 20 min when the acid-base environment is varying. When the grid number reached 132511 and beyond, the variations of average velocity (see Fig. 3(a)), average pH (see Fig. 3(b)) and concentration distribution of sodium bicarbonate (see Fig. 3(c)) were not significant with the increase of grid number. Therefore, a grid number of 132511 was adopted for simulation.

3.2. Comparison of different secretory modes

The effects of different secretion modes on the mass transfer and mixing in the duodenum were investigated by implementing the three cases listed in Table 2. Fig. 4 shows the distribution of velocity streamlines in one cycle of segmentation movement in the duodenum. The black arrows indicate vortexes. The pancreaticobiliary port is indicated by a thick blue arrow.

For the base case (see Fig. 4(a)), the maximum velocity of the flow field obtained from the simulation was 0.003 $m \cdot s^{-1}$, which is in the range of the measured average velocity of chyme flow in the human intestine (0.0002 – 0.005 $m \cdot s^{-1}$) [26]. The intestinal wall contracts to a maximum amplitude at $T/4$, where T is the cycle period of one segmentation movement. This movement leads to a symmetrical distribution of vortices in the relaxation area. At $T/2$, the intestinal shape returns to its initial state, and the symmetric vortices disappear. The flow velocity in the original relaxation region becomes relatively higher due to the inward extrusion by the wall. In the second half of the cycle, one can see an opposite evolution of velocity field. When the wall secretion is discarded (see Fig. 4(b)), the jet flow from the pancreaticobiliary port becomes very strong to disturb its nearby vortex. It may go against the acid-base mixing because the vortex is expected to promote the transport of the pancreaticobiliary secretion toward the intestinal entrance as illustrated in Fig. 4(a). In comparison, the

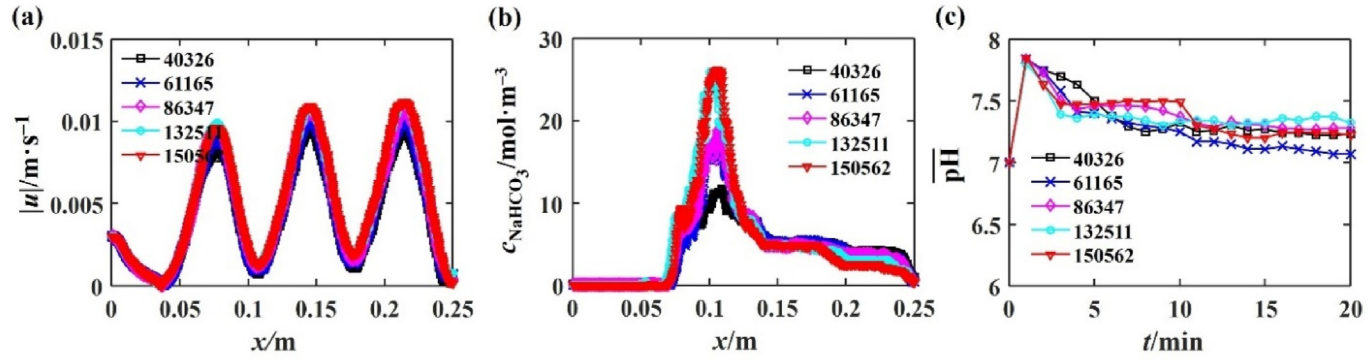

Fig. 3. Simulation results obtained under different meshes: (a) the distribution of velocity magnitude along the axis at 20 min; (b) concentration distribution of sodium bicarbonate along the axis at 20 min; (c) evolution of average pH over time.

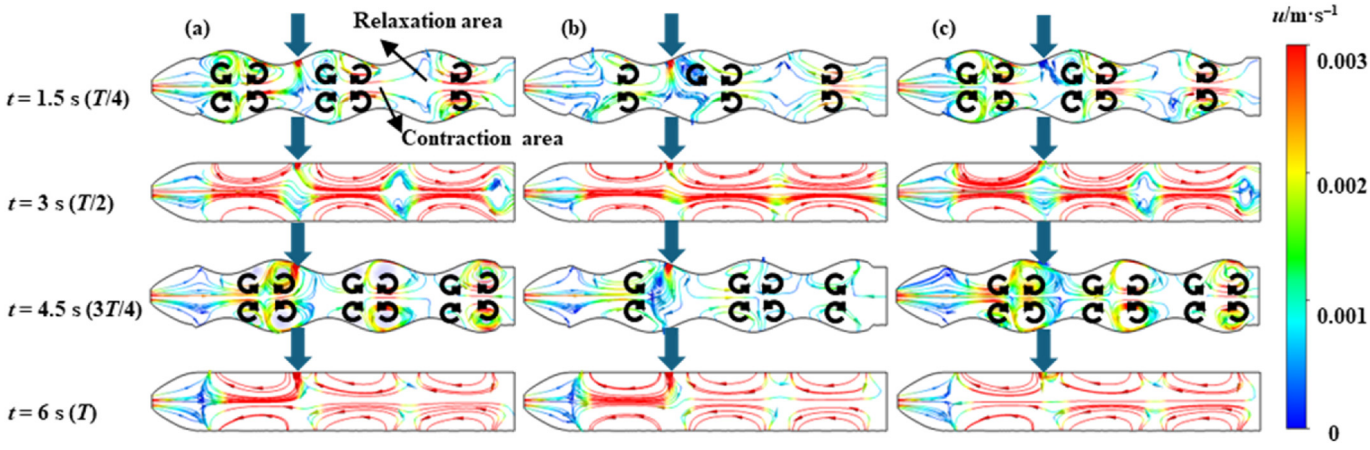

Fig. 4. The distribution of velocity fields in one cycle of segmentation movement: (a) base case; (b) pancreaticobiliary secretion only; and (c) wall secretion only.

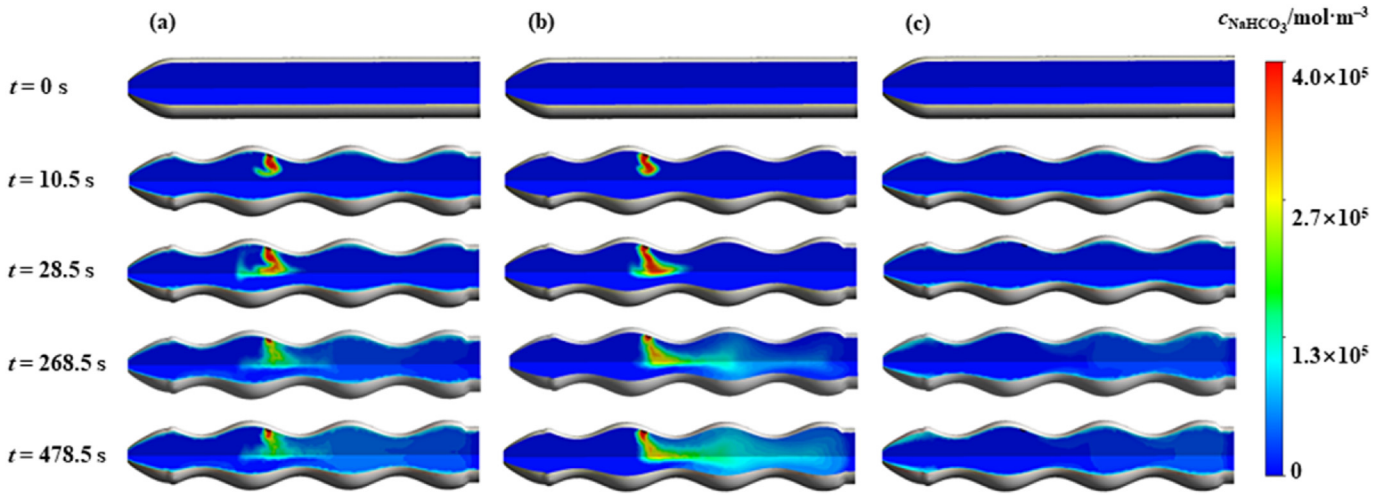

Fig. 5. Evolution of concentration fields over time: (a) base case; (b) pancreaticobiliary secretion only; (c) wall secretion only.

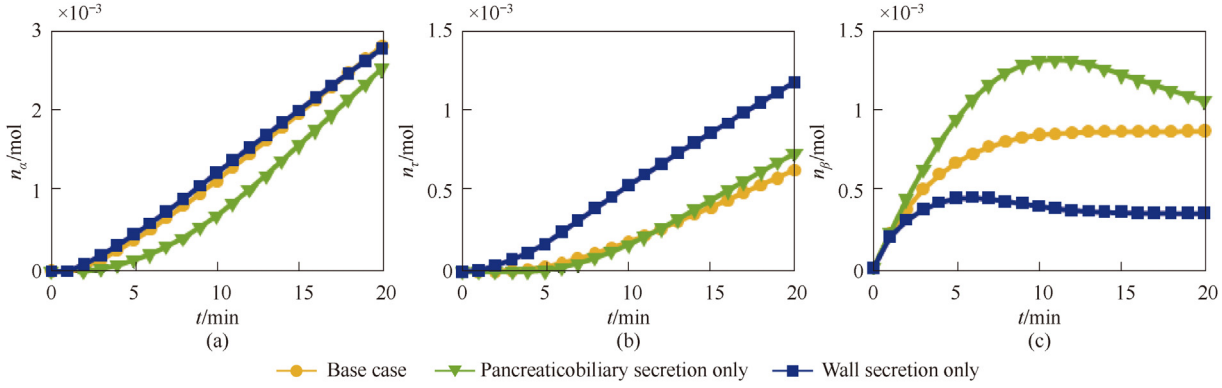

Fig. 6. Evolution of the amount of sodium bicarbonate over time (a) consumed by hydrochloric acid in the lumen, (b) discharged from the intestine, and (c) remained in the lumen.

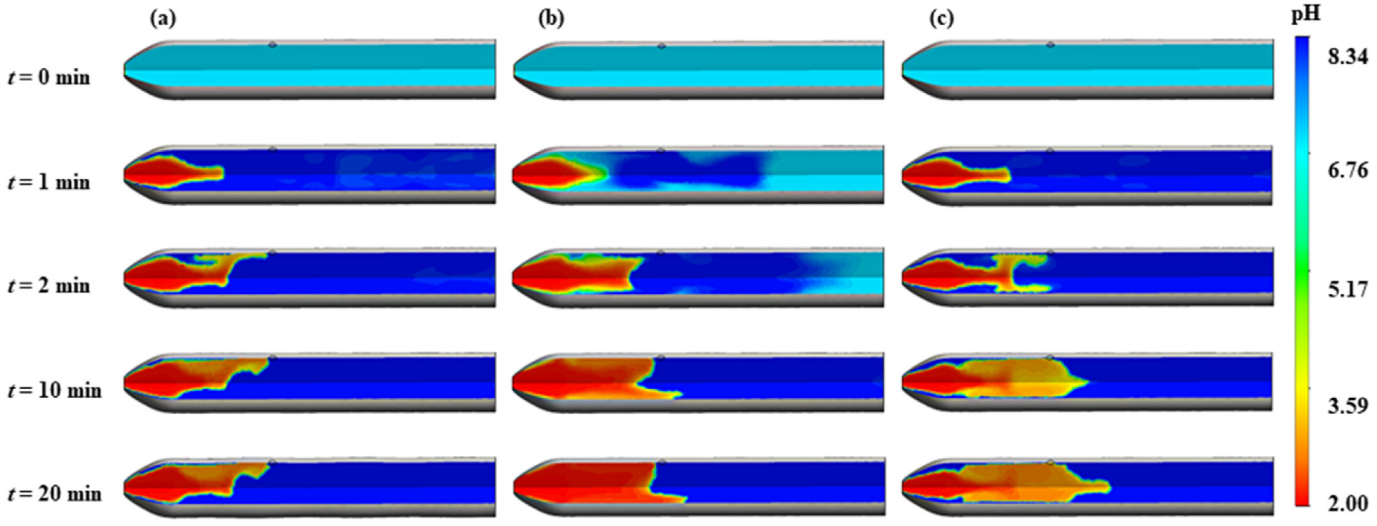

Fig. 7. Spatial distribution of pH in the intestinal lumen over time: (a) base case; (b) pancreaticobiliary secretion only; and (c) wall secretion only.

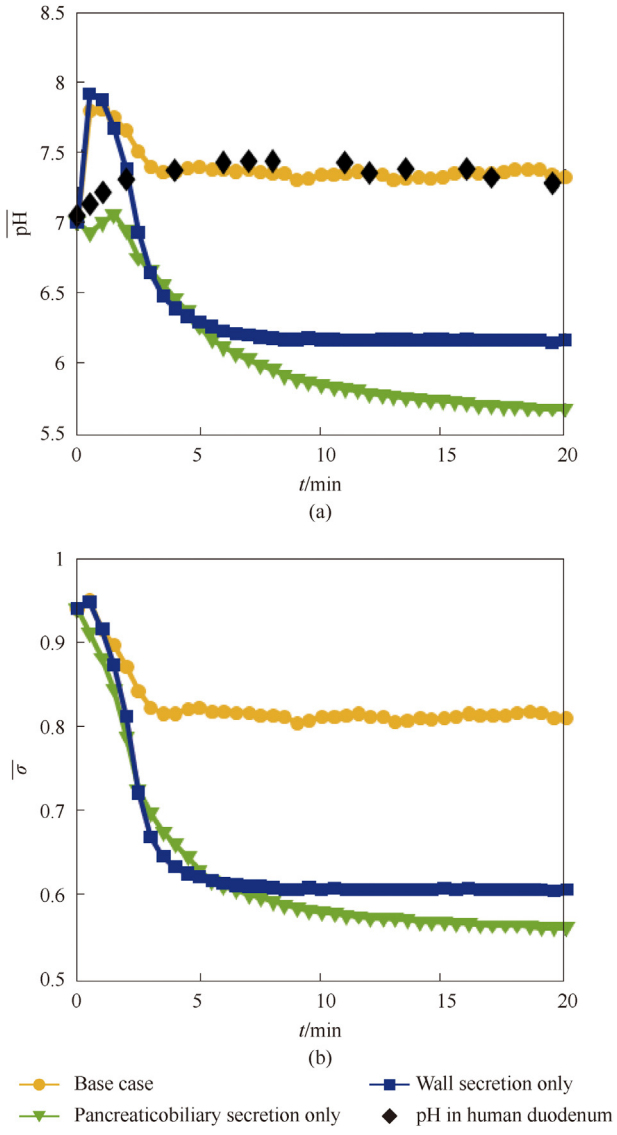

Fig. 8. Evolution of (a) average pH and (b) average enzyme activity in the intestine over time. (The experimental data in the graph are from the study of Maurer *et al.* [47].).

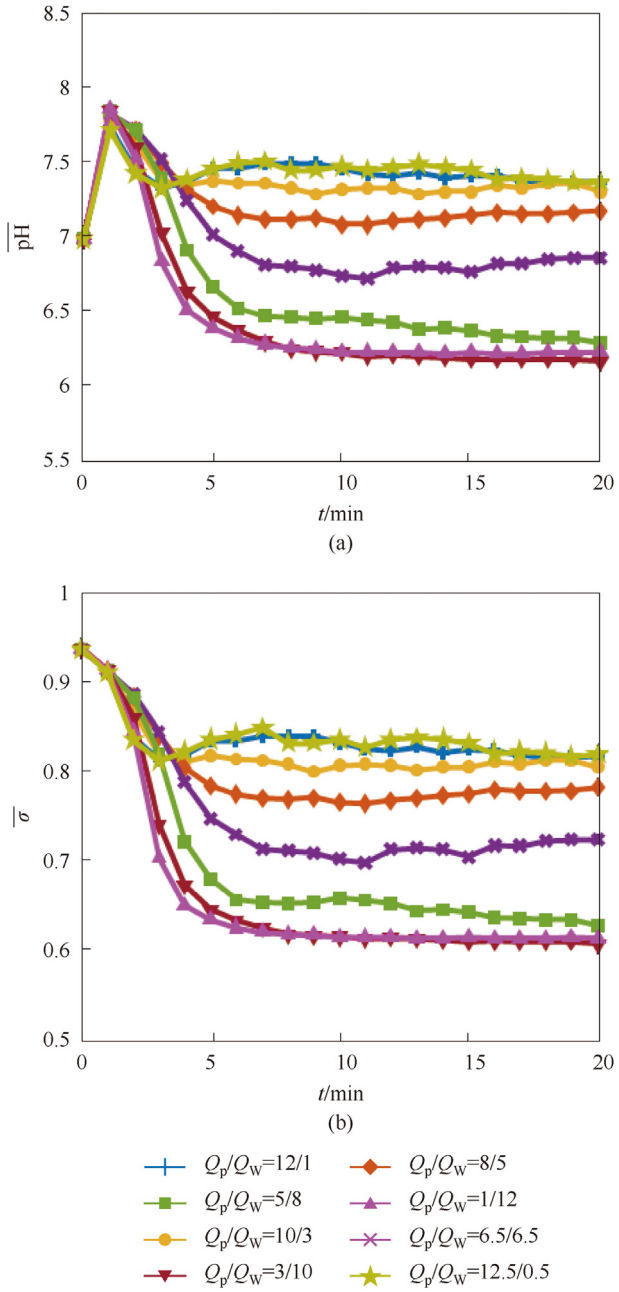

Fig. 9. Effect of the ratio of pancreaticobiliary secretion to wall secretion on (a) average pH, and (b) average enzyme activity in the intestine.

disappearance of the pancreaticobiliary secretion in Fig. 4(c) has a negligible effect on the flow of the chyme.

Fig. 5 illustrates the distribution of sodium bicarbonate concentration in the intestine over time. Fig. 6 shows temporal evolutions of three states of sodium bicarbonate, including consumed by neutralization reaction, remained in the duodenum and escaped from the outlet. In the base case (see Fig. 5(a)), the alkaline fluid secreted from the pancreaticobiliary port spreads in both directions, accelerating its contact with the acid solution from the stomach. In comparison, the sodium bicarbonate in the case with pancreaticobiliary secretion solely (see Fig. 5(b)) demonstrates a trend to transport downward. The above phenomena can be used to understand results depicted in Fig. 6. When the system has pancreaticobiliary secretion only, the consumption of sodium bicarbonate due to reaction is inhibited, and the loss resulting from discharging goes up.

As shown in Fig. 5(c), wall-only secretion creates solely a thin layer of sodium bicarbonate close to the inner surface of the tube. In Fig. 6(c), this case exhibits relatively lower amount of sodium bicarbonate remained in the lumen, which could be understood from two aspects. According to the design for case study, excluding the secretion from the pancreaticobiliary port means a higher amount of the wall secretion. On the one hand, more sodium bicarbonate is consumed by acidic gastric juice in the region close to the entrance, in particular during the initial period (see Fig. 6(a)). On the other hand, secretion in the posterior part is easier to flow out of the tract, as given in Fig. 6(b).

The distribution of pH in the intestine over time is depicted in Fig. 7. The expansion of the acidic region in the base case is slowest among the three cases. It can be explained based on the analyses of the velocity fields and concentration fields above. The base case system possesses both two secretion modes, which can offer a relatively higher intensity of vortex that promotes the acid-base

mixing and neutralizing reaction. For the case of pancreaticobiliary secretion only, the sodium bicarbonate in the intestinal lumen is the most (see Fig. 6(c)), but this secretion mode is not conducive to neutralization with acidic gastric juices. Thus, the ability of intestinal fluid to neutralize gastric acid is strongest when two secretion modes coexist. As plotted in Fig. 8(a), the average pH in the base case is maintained at a relatively high level. The simulation results for the base case are almost consistent with the data measured in a previous *in-vivo* experiment, where 16 healthy volunteers swallowed IntelliCap capsules after a meal, demonstrating the effectiveness of the model [47]. However, a drastic growth of the simulated average pH in the early stage was not observed in that experiment. It may be attributed to the limitation of the experimental technology that can only measure the pH value at a specific position instead of the average level throughout the entire duodenum. Especially at the very beginning, the neutralization taken place near the entrance could not be captured by experimental measurement. Therefore, this numerical method has the advantage of obtaining more comprehensive details in the digestive tract.

The activity of pancreatic lipase, which is the major enzyme for breaking down fat, is evaluated based on Eq. (15). Fig. 8(b) shows the evolution of average activity with time for the three cases. It can be found that their trends are basically consistent with those of the average pH (see Figs. 8(a) and 9(a)). When the two secretion modes coexist, the average enzyme activity remains stable at a very high level, about 80%, as pancreatic lipase is an enzyme which is most active in a near-neutral environment [40]. In contrast, the activity of lipase in other two cases is inhibited to a large extent.

3.3. Effect of the proportion of the two secretion modes Q_p/Q_w

The simulation results in the previous section reveal that the coexistence of the two secretion modes can greatly promote the acid-base reaction in the tract, and consequently provide a superior pH environment for lipase digestion. It raises an intriguing question: what is the optimal proportion of pancreaticobiliary secretion to wall secretion? Eight cases differing in this proportion were conducted to investigate its effect.

Fig. 9 shows the average pH and the average lipase activity in the lumen, respectively. When the Q_p/Q_w is in the range of 10/3 – 12.5/0.5, the trend of pH change and the pH value at around 20 min are very close. The simulation results obtained for these conditions are in general agreement with the data measured in the *in vivo* experiment mentioned above in which 16 healthy volunteers swallowed IntelliCap capsules after a meal [47]. This suggests that a ratio of 10/3 – 12.5/0.5 is a suitable ratio range of the two secretory modes, providing a suitable pH environment in the gut. When Q_p/Q_w is 1/12 – 5/8, a dramatic reduction in pH tells that the ability of intestinal secretion to neutralize gastric acid is significantly deteriorated. For patients with exocrine pancreatic insufficiency, the decrease in the ration of pancreaticobiliary secretion, causing the Q_p/Q_w to be out of the optimal range, lowers the average intestinal pH, even far below the physiological level in a normal human. This phenomenon was also observed by Dimagno *et al.* [48] in patients with pancreatitis.

As shown in Fig. 9(b), trends in pH and average enzyme activity are consistent. The conditions within the optimal range of Q_p/Q_w (10/3 – 12.5/0.5) provides a suitable environment for the survival of lipase. And its average enzyme activity is basically more than 80%. In contrast, in the range of Q_p/Q_w (1/12 – 5/8), the average enzyme activity reduces to 0.6, suggesting that an imbalanced acid-base environment in this range leads to an imbalance in the conditions for lipase survival. Additionally, a more acidic environment gives rise to a decline in the average activity of lipase. As a result, fat in the duodenum cannot be digested in time. Patients with exocrine pancreatic insufficiency are prone to suffer from functional dyspepsia and malnutrition [49] and take pancreatic enzyme preparations to enhance the intestinal concentration. From the simulation results, acid suppressants that can ease the acidic intestinal environment for digestive enzymes could be an alternative treatment method. A potential choice, for example, is proton pump inhibitor, which has been widely used in the treatment of diseases such as acute pancreatitis and are effective in clinical practice [50].

4. Conclusions

This study developed a preliminary 3D duodenum model taking both pancreaticobiliary secretion and wall secretion into account. The effects of these two secretion modes on the intestinal environment were analyzed comprehensively by comparing fluid flow, mass transfer and pH variation. When two secretion modes coexist, higher allocation of pancreaticobiliary secretion is capable of creating a more conducive *in-vivo* environment for lipase digestion. However, the deficiency of each mode impairs the neutralization ability of intestinal fluid to gastric acid, and consequently suppresses the activity of lipase.

Beyond providing valuable insights into intestinal physiology and associated diseases, our numerical simulations of the intestine have the potential to inspire advancements in the design of bio-inspired soft reactors for process intensification. For instance, simulation results demonstrate that peristaltic motion applied to the intestinal wall significantly enhances mixing efficiency. Unlike conventional agitation techniques, this novel mixing mechanism generates a gently sheared environment, which is particularly advantageous for preserving shear-sensitive microorganisms involved in the process. Additionally, the findings related to liquid injection modes within the intestine can guide the design of more effective jet injection systems in chemical reactors. This approach enables a more uniform distribution of reactants, minimizes dead zones, and enhances overall reaction efficiency.

It should be pointed out that the model established in this work is currently different from a real intestine in many ways. Some unique physiological features, *e.g.,* curved geometry, wall microstructures and absorption, have not been taken into account. The absorption function, in particular, is likely to affect the electrolyte concentration. The contents in the intestine are composed of liquid, gas and even solid in most cases. A multi-phase flow simulation should be conducted in the future. Moreover, a comprehensive gastro-duodenum model is currently being developed by integrating separate models for the stomach and duodenum [51–54]. Regulatory mechanisms of bicarbonate secretion, such as feedback control in response to pH levels in the intestinal lumen, should also be incorporated as our understanding of these processes improves. Anyway, this work makes the first effort to incorporate a comprehensive secretory system into an in-silico intestine model.

CRediT Authorship Contribution Statement

Yulan Zhao: Writing – original draft, Visualization, Validation, Software, Methodology, Investigation, Formal analysis. Yifan Qin: Writing – original draft, Visualization, Validation, Software, Methodology, Formal analysis. Xiao Dong Chen: Supervision, Conceptualization. Jie Xiao: Writing – review & editing, Validation, Supervision, Project administration, Methodology, Investigation, Funding acquisition, Formal analysis, Conceptualization.

Declaration of Competing Interest

The authors declare that they have no known competing financial interests or personal relationships that could have appeared to influence the work reported in this paper.

Acknowledgements

We are grateful for the financial support from the National Natural Science Foundation of China (21978184), the “Jiangsu Innovation and Entrepreneurship (Shuang Chuang) Program”, the “Jiangsu Specially-Appointed Professors Program”, and the “Priority Academic Program Development (PAPD) of Jiangsu Higher Education Institutions”.

References

[1] M.A.J.S. van Boekel, Kinetic Modeling of Reactions in Foods, CRC Press, Boca Raton, 2009.
[2] D.M. Mudie, G.L. Amidon, G.E. Amidon, Physiological parameters for oral delivery and *in vitro* testing, *Mol. Pharm.* 7 (5) (2010) 1388–1405.
[3] W. Woodtli, C. Owyang, Duodenal pH governs interdigestive motility in humans, *Am. J. Physiol.* 268 (1 Pt 1) (1995) G146–G152.
[4] J.E. Hall, Guyton and Hall: Textbook of Medical Physiology, Elsevier Saunders, Philadelphia, 2016.
[5] E.N. Marieb, S.M. Keller, Essentials of Human Anatomy & Physiology, Pearson, New York, 2017.
[6] L. Sherwood, Fundamentals of Human Physiology, Brooks/Cole Cengage Learning, Canada, 2012.
[7] M.E. Smith, D.G. Morton, The Digestive System, Churchill Livingstone, Edinburgh, 2010.
[8] H. Glad, M.A. Ainsworth, P. Svendsen, J. Fahrenkrug, O.B. Schaffalitzky de Muckadell, Effect of vasoactive intestinal peptide and pituitary adenylate cyclase-activating polypeptide on pancreatic, hepatic and duodenal mucosal bicarbonate secretion in the pig, *Digestion* 67 (1–2) (2003) 56–66.
[9] S.K. Dutta, R.M. Russell, F.L. Iber, Influence of exocrine pancreatic insufficiency on the intraluminal pH of the proximal small intestine, *Dig. Dis. Sci.* 24 (7) (1979) 529–534.
[10] S.K. Dutta, R.M. Russell, F.L. Iber, Impaired acid neutralization in the duodenum in pancreatic insufficiency, *Dig. Dis. Sci.* 24 (10) (1979) 775–780.
[11] L. Ovesen, F. Bendtsen, U. Tage-Jensen, N.T. Pedersen, B.R. Gram, S.J. Rune, Intraluminal pH in the stomach, duodenum, and proximal jejunum in normal subjects and patients with exocrine pancreatic insufficiency, *Gastroenterology* 90 (4) (1986) 958–962.
[12] J.I. Isenberg, D.L. Hogan, F.J. Thomas, Duodenal mucosal bicarbonate secretion in humans: a brief review, *Scand. J. Gastroenterol.* 21 (sup125) (1986) 106–112.
[13] J.I. Isenberg, J.A. Selling, D.L. Hogan, M.A. Koss, Impaired proximal duodenal mucosal bicarbonate secretion in patients with duodenal ulcer, *N. Engl. J. Med.* 316 (7) (1987) 374–379.
[14] E.M. Quigley, L.A. Turnberg, pH of the microclimate lining human gastric and duodenal mucosa *in vivo*. Studies in control subjects and in duodenal ulcer patients, *Gastroenterology* 92 (6) (1987) 1876–1884.
[15] J.D. Wolosin, F.J. Thomas, D.L. Hogan, M.A. Koss, T.M. O'Dorisio, J.I. Isenberg, The effect of vasoactive intestinal peptide, secretin, and glucagon on human duodenal bicarbonate secretion, *Scand. J. Gastroenterol.* 24 (2) (1989) 151–157.
[16] H.S. Odes, D.L. Hogan, M.A. Ballesteros, J.D. Wolosin, M.A. Koss, J.I. Isenberg, Human duodenal mucosal bicarbonate secretion. Evidence suggesting active transport under basal and stimulated conditions, *Gastroenterology* 98 (4) (1990) 867–872.
[17] M.A. Ballesteros, J.D. Wolosin, D.L. Hogan, M.A. Koss, J.I. Isenberg, Cholinergic regulation of human proximal duodenal mucosal bicarbonate secretion, *Am. J. Physiol.* 261 (2 Pt 1) (1991) G327–G331.
[18] F. Bendtsen, B. Rosenkilde-Gram, U. Tage-Jensen, L. Ovesen, S.J. Rune, Duodenal bulb acidity in patients with duodenal ulcer, *Gastroenterology* 93 (6) (1987) 1263–1269.
[19] M.A. Ainsworth, J. Kjeldsen, O. Olsen, P. Christensen, O.B. Schaffalitzky de Muckadell, Duodenal disappearance rate of acid during inhibition of mucosal bicarbonate secretion, *Digestion* 47 (3) (1990) 121–129.
[20] M.A. Ainsworth, P. Svendsen, H. Glad, N.J. Andersen, O. Olsen, O.B. Schaffalitzky de Muckadell, Duodenal mucosal bicarbonate secretion in pigs is accompanied by compensatory changes in pancreatic and biliary HCO_3^- secretion, *Scand. J. Gastroenterol.* 29 (10) (1994) 889–896.
[21] J.S. Karthikeyan, D. Salvi, M.G. Corradini, R.D. Ludescher, M.V. Karwe, Effect of bolus viscosity on carbohydrate digestion and glucose absorption processes: an in vitro study, *Physics of Fluids* 31 (11) (2019) 111905.
[22] O. Gouseti, M.R. Jaime-Fonseca, P.J. Fryer, C. Mills, M.S.J. Wickham, S. Bakalis, Hydrocolloids in human digestion: dynamic *in-vitro* assessment of the effect of food formulation on mass transfer, *Food Hydrocoll.* 42 (2014) 378–385.
[23] R.P. Deng, C. Selomulya, P. Wu, M.W. Woo, X.E. Wu, X.D. Chen, A soft tubular model reactor based on the bionics of a small intestine–Starch hydrolysis, *Chem. Eng. Res. Des.* 112 (2016) 146–154.
[24] H. Ishiguro, A. Yamamoto, M. Nakakuki, L.J. Yi, M. Ishiguro, M. Yamaguchi, S. Kondo, Y. Mochimaru, Physiology and pathophysiology of bicarbonate secretion by pancreatic duct epithelium, *Nagoya J. Med. Sci.* 74 (1–2) (2012) 1–18.
[25] S. Clarysse, J. Tack, F. Lammert, G. Duchateau, C. Reppas, P. Augustijns, Postprandial evolution in composition and characteristics of human duodenal fluids in different nutritional states, *J. Pharmaceut. Sci.* 98 (3) (2009) 1177–1192.
[26] B. Hens, Y. Tsume, M. Bermejo, P. Paixao, M.J. Koenigsknecht, J.R. Baker, W.L. Hasler, R. Lionberger, J.H. Fan, J. Dickens, K. Shedden, B. Wen, J. Wysocki, R. Loebenberg, A. Lee, A. Frances, G. Amidon, A. Yu, G. Benninghoff, N. Salehi, A. Talattof, D.X. Sun, G.L. Amidon, Low buffer capacity and alternating motility along the human gastrointestinal tract: implications for *in vivo* dissolution and absorption of ionizable drugs, *Mol. Pharm.* 14 (12) (2017) 4281–4294.
[27] J. Al-Gousous, K.X. Sun, D.P. McNamara, B. Hens, N. Salehi, P. Langguth, M. Bermejo, G.E. Amidon, G.L. Amidon, Mass transport analysis of the enhanced buffer capacity of the bicarbonate-CO_2 buffer in a phase-heterogenous system: physiological and pharmaceutical significance, *Mol. Pharm.* 15 (11) (2018) 5291–5301.
[28] T. Zhu, A. Xia, K. Lin, Y. Huang, X.Q. Zhu, X. Zhu, Q. Liao, Numerical investigation of bio-inspired mixing enhancement for enzymatic hydrolysis, *Chem. Eng. Sci.* 260 (2022) 117950.
[29] P.V. Trusov, N.V. Zaitseva, M.R. Kamaltdinov, A multiphase flow in the antroduodenal portion of the gastrointestinal tract: a mathematical model, *Comput. Math. Methods Med.* 2016 (2016) 5164029.
[30] M.R. Kamaltdinov, Multi-component mixture flow in the stomach and duodenum allowing for functional disorders: results of numeric modelling for determining acidity, *Russ. J. Biomech.* 20 (3) (2017) 23–34.
[31] C.H. Sun, X.H. Li, T. Chan, Z.P. Peng, Z. Dong, Y.J. Luo, Z.P. Li, S.T. Feng, Multidetector computed tomography (MDCT) manifestations of the normal duodenal papilla, *Eur. J. Radiol.* 82 (6) (2013) 918–922.
[32] N. Palmada, S. Hosseini, R. Avci, J.E. Cater, V. Suresh, L.K. Cheng, A systematic review of computational fluid dynamics models in the stomach and small intestine, *Appl. Sci.* 13 (10) (2023) 6092.
[33] K. Järbur, J. Dalenbäck, H. Sjövall, Quantitative assessment of motility-associated changes in gastric and duodenal luminal pH in humans, *Scand. J. Gastroenterol.* 38 (4) (2003) 392–398.
[34] K. Barrett, S. Barman, S. Boitano, H. Brooks, Overview of Gastrointestinal Function & Regulation. Ganong's Review of Medical Physiology, McGraw-Hill Education, the United States, 2015.
[35] J.M. Froehlich, M.A. Patak, C. von Weymarn, C.F. Juli, C.L. Zollikofer, K.U. Wentz, Small bowel motility assessment with magnetic resonance imaging, *J. Magn. Reson. Imag.* 21 (4) (2005) 370–375.
[36] N.D. Wright, F.B. Kong, B.S. Williams, L. Fortner, A human duodenum model (HDM) to study transport and digestion of intestinal contents, *J. Food Eng.* 171 (2016) 129–136.
[37] S.J. Pandol, The Exocrine Pancreas, BMJ Group, UK, 2010.
[38] O.L. Lewis, J.P. Keener, A.L. Fogelson, A physics-based model for maintenance of the pH gradient in the gastric mucus layer, *Am. J. Physiol. Gastrointest. Liver Physiol.* 313 (6) (2017) G599–G612.
[39] M. Eigen, G.G. Hammes, Elementary steps in enzyme reactions (as studied by relaxation spectrometry), *Adv. Enzymol. Relat. Subj. Biochem.* 25 (1963) 1–38.
[40] M. Sémériva, C. Dufour, P. Desnuelle, On the probable involvement of a histidine residue in the active site of pancreatic lipase, *Biochemistry* 10 (11) (1971) 2143–2149.
[41] R.G. Lentle, P.W.M. Janssen, The Physical Processes of Digestion, Springer, New York, 2011.
[42] B.J. Krieg, S.M. Taghavi, G.L. Amidon, G.E. Amidon, *In vivo* predictive dissolution: transport analysis of the CO_2, bicarbonate *in vivo* buffer system, *J. Pharmaceut. Sci.* 103 (11) (2014) 3473–3490.
[43] I. Locatelli, A. Mrhar, M. Bogataj, Gastric emptying of pellets under fasting conditions: a mathematical model, *Pharm. Res.* 26 (7) (2009) 1607–1617.
[44] C.H. You, J.M. Rominger, W.Y. Chey, Potentiation effect of cholecystokinin-octapeptide on pancreatic bicarbonate secretion stimulated by a physiologic dose of secretin in humans, *Gastroenterology* 85 (1) (1983) 40–45.
[45] W. Ganong, Review of medical physiology, *Comp. Biochem. Physiol.* 12 (2023) 40–67.
[46] H.H. Sky-Peck, P. Thuvasethakul, Human pancreatic alpha-amylase. II. Effects of pH, substrate and ions on the activity of the enzyme, *Ann. Clin. Lab. Sci.* 7 (4) (1977) 310–317.
[47] J.M. Maurer, R.C. Schellekens, H.M. van Rieke, C. Wanke, V. Iordanov, F. Stellaard, K.D. Wutzke, G. Dijkstra, M. van der Zee, H.J. Woerdenbag, H.W. Frijlink, J.G. Kosterink, Gastrointestinal pH and transit time profiling in healthy volunteers using the IntelliCap system confirms ileo-colonic release of ColoPulse Tablets, *PLoS One* 10 (7) (2015) e0129076.
[48] E.P. DiMagno, Gastric acid suppression and treatment of severe exocrine pancreatic insufficiency, *Best Pract. Res. Clin. Gastroenterol.* 15 (3) (2001) 477–486.
[49] A. Hedström, C. Steiner, R. Valente, S.L. Haas, J.M. Löhr, M. Vujasinovic, Pancreatic exocrine insufficiency and Crohn's disease, *Minerva Gastroenterol. Dietol.* 66 (1) (2020) 17–22.
[50] J. Cai, W. Zhou, H.S. Luo, L.V. Peng, Effect of proton pump inhibitor on amylase release from isolated pancreatic acini, *In Vitro Cell. Dev. Biol. Anim.* 43 (1) (2007) 25–27.

[51] J.P. Zha, S.Y. Zou, J.Y. Hao, X.J. Liu, G. Delaplace, R. Jeantet, D. Dupont, P. Wu, X. D. Chen, J. Xiao, The role of circular folds in mixing intensification in the small intestine: a numerical study, *Chem. Eng. Sci.* 229 (2021) 116079.
[52] Y.N. Zhang, P. Wu, R. Jeantet, D. Dupont, G. Delaplace, X.D. Chen, J. Xiao, How motility can enhance mass transfer and absorption in the duodenum: taking the structure of the villi into account, *Chem. Eng. Sci.* 213 (2020) 115406.
[53] C. Li, J. Xiao, X.D. Chen, Y. Jin, Mixing and emptying of gastric contents in human-stomach: a numerical study, *J. Biomech.* 118 (2021) 110293.
[54] Y.F. Qin, J. Xiao, A.B. Yu, X.D. Chen, Numerical investigation of starch-based granular food digestion in the duodenum: the role of duodenal posture and gastric acidity, *Chem. Eng. J.* 500 (2024) 156965.